

# Technical Notes

## Theoretical Modeling of the Chemical Non-Equilibrium Flow Behind a Normal Shock Wave

Zhihui Wang,\* Lin Bao,† and Binggang Tong‡  
Graduate University of Chinese Academy of Sciences,  
100049 Beijing, People's Republic of China

DOI: 10.2514/1.J051044

### Nomenclature

$d$	=	molecular diameter, $4.17 \times 10^{-10}$ for $N_2$ and $3.0 \times 10^{-10}$ for $N$ at $T_{ref}$ , m
$k$	=	Boltzmann constant, $1.38 \times 10^{-23}$ , J/K
$k_f$	=	dissociation reaction rate, $m^3/(molecule \cdot s)$
$k_r$	=	recombination reaction rate, $m^6/(molecule^2 \cdot s)$
$M$	=	Mach number
$m$	=	molecular mass, $46.5 \times 10^{-27}$ for $N_2$ , kg
$n$	=	number density, molecule/m <sup>3</sup>
$R$	=	specific gas constant, 297 for $N_2$ , J/kg · K
$T$	=	temperature, K
$U_\infty$	=	free-stream velocity, m/s
$u$	=	velocity of the flow, m/s
$x$	=	distance downstream the shock wave, m
$\alpha$	=	degree of dissociation
$\theta_d$	=	characteristic dissociation temperature, 113,500 for $N_2$ , K
$\theta_v$	=	characteristic vibration temperature, 3371 for $N_2$ , K
$\lambda$	=	molecular mean free path, $(T/T_{ref})^\omega / (\sqrt{2\pi} d_{ref}^2 n)$ , m
$\mu$	=	nondimensional kinetic energy, $U_\infty^2 / (2R\theta_d)$
$\rho$	=	density, kg/m <sup>3</sup>
$\rho_d$	=	characteristic density, kg/m <sup>3</sup>
$\sigma$	=	collision cross section, m <sup>2</sup>
$\dot{\Omega}$	=	chemical reaction source term, molecule/m <sup>3</sup> · s
$\omega$	=	viscosity-temperature index, 0.75 for $N_2$ and $N$
$\zeta_v$	=	vibrational degree of freedom, $2(\theta_v/T)/[\exp(\theta_v/T) - 1]$

### Subscripts and superscript

$e$	=	equilibrium value
ref	=	reference value at $T_{ref} = 273.15$ K

Received 9 November 2010; revision received 6 August 2011; accepted for publication 18 August 2011. Copyright © 2011 by the American Institute of Aeronautics and Astronautics, Inc. All rights reserved. Copies of this paper may be made for personal or internal use, on condition that the copier pay the \$10.00 per-copy fee to the Copyright Clearance Center, Inc., 222 Rosewood Drive, Danvers, MA 01923; include the code 0001-1452/12 and \$10.00 in correspondence with the CCC.

\*Ph.D. Candidate, College of Physical Sciences, Graduate University of Chinese Academy of Sciences, 19(A) Yuquan Road, 100049 Beijing, People's Republic of China.

†Associate Professor, College of Physical Sciences, Graduate University of Chinese Academy of Sciences, 19(A) Yuquan Road, 100049 Beijing, People's Republic of China.

‡Professor, College of Physical Sciences, Graduate University of Chinese Academy of Sciences, 19(A) Yuquan Road, 100049 Beijing, People's Republic of China; tongbg@gucas.ac.cn.

\* = nondimensional quantity  
∞ = free-stream condition in front of the shock wave

### I. Introduction

THE nonequilibrium flow behind a strong normal shock wave is a typical and classical topic for discussion. However, so far it is still unrealizable to directly and explicitly predict the postshock nonequilibrium features based on the free-stream parameters in front of the shock wave. An in-depth exploration is very necessary, considering the important role of this problem in both the theoretical research field and the engineering practice.

A very useful theoretical tool to study this problem is the ideal dissociating gas (IDG) model, which was established by Lighthill [1] and Freeman [2] about half a century ago. By introducing the concept of the degree of dissociation in a dissociation-recombination reaction, they built the conservation equations and the state equation for a nonequilibrium dissociating gas, which greatly simplified the analysis and calculation on the nonequilibrium flow field behind a shock wave. They also approximately analyzed the equilibrium degree of dissociation and nonequilibrium characteristic scale by using the semi-analytical and seminumerical method.

Subsequently, based on this theoretical model, many other scholars [3–6] have carried on further or more in-depth analyses on the related flow problems. Besides, the numerical methods, such as the computational fluid dynamics (CFD) [7–9] and the direct simulation Monte Carlo (DSMC) method [10–12], have also been widely used. However, whereas the numerical methods are excessively relied upon, there is still no clear and sophisticated theoretical conclusion on the relationship between the pre- and postshock parameters.

In this paper, the IDG model will be followed to theoretically explore the explicit analytical relationship between the postshock nonequilibrium characteristics and the preshock free-stream condition of the flow. Taking the nitrogen gas as a typical example, a dissociation-recombination reaction rate equation based on the molecular kinetic theory is built. After some appropriate physical analysis and mathematical simplifications, the explicit expression of the equilibrium degree of dissociation and the nonequilibrium characteristic scale are obtained. Then a detailed parameter analysis is carried out and an intuitive formula that can approximately give a normalized description of the nonequilibrium flow field behind a shock wave is found. Finally, results of the present study are verified with DSMC results and other experimental and numerical data.

The present study has both theoretical significance and practical value. On one side, it may be the more detailed and substantial result so far to improve understanding of the nonequilibrium flow behind a strong shock wave, and it is helpful to enrich the theoretical framework of this classical problem. On the other side, the conclusions in this paper provide specific guidance for a fast estimation of the nonequilibrium flow field in a hypersonic wind tunnel and for the analysis of experimental or CFD results.

### II. Problem Description and Modeling

Figure 1 shows the main features of a chemical nonequilibrium flow behind a strong normal shock wave. Physically speaking, all the flow field details behind the shock wave are completely determined by the preshock free-stream conditions. For a perfect gas or the frozen case, the temperature, pressure, and density behind the shock wave can be directly determined from the Rankine-Hugoniot theory. However, in many real problems, the gas is not ideal or perfect and real gas effects play an important role. For diatomic gases, such as nitrogen, oxygen, and equivalent air, high temperature will cause the

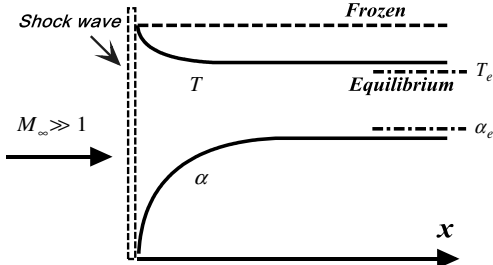


Fig. 1 Schematic of the chemical nonequilibrium flow behind a normal shock wave.

molecules to vibrate, dissociate, or even ionize. In turn, these effects absorb energy and decrease the temperature. The physical quantities undergo a nonequilibrium process, rapidly varying near the shock wave and slowly approaching the equilibrium limits at infinity, where the molecular recombination and dissociation counteract with each other. The final equilibrium state and the specific transient process completely depend on the free-stream condition in front of the shock wave. The main purpose of this paper is to find the mathematical relationship between them and to analyze how it works.

Before further discussion, two appropriate statements need to be made. First, as a typical flow model, only the flow behind the shock wave is concerned, whereas what happens in the narrow zone of shock wave will not be discussed. It is also assumed that the free-stream temperature is relatively so low that no molecules dissociate in front of the shock wave. Second, the influence of the thermal nonequilibrium, including the molecular vibrational nonequilibrium, is not so important in comparison with that of the chemical nonequilibrium. Therefore, an ensemble approximation to the vibrational degree of freedom is introduced here, whereas a constant value equaling 1.0 was employed by Freeman [2].

The dissociation-recombination reaction of the nitrogen gas is considered as



in which  $\Upsilon$  represents an intermediate molecule, being  $N_2$  or  $N$ . The degree of dissociation equals the mass fraction of the dissociated gas. Therefore,

$$\alpha = \rho_N / (\rho_{N_2} + \rho_N) = \rho_N / \rho \quad (2)$$

Its equilibrium value  $\alpha_e$  is obtained when the flow reaches the equilibrium state. The nonequilibrium characteristic scale is defined as the distance required to reach 95% of the equilibrium degree of dissociation, i.e.,  $\alpha = 0.95\alpha_e$  at  $x = x_e$ .

As a one-dimensional flow model, all the mass, momentum, and energy of the flow are conservative downstream the shock wave. The nondimensional conservation equations of the gas are expressed as

$$\rho^* u^* = 1 \quad (3a)$$

$$(1 + \alpha) \rho^* T^* / (2\mu) + \rho^* (u^*)^2 \approx 1 \quad (3b)$$

$$(4 + \alpha) T^* + T^* (\zeta_v - 1) (1 - \alpha) / 2 + \alpha + \mu (u^*)^2 \approx \mu \quad (3c)$$

where the nondimensional quantities are defined as  $\rho^* = \rho / \rho_\infty$ ,  $u^* = u / U_\infty$ , and  $T^* = T / \theta_d$ .

To facilitate further discussion, some appropriate approximations to the conservation equations are needed, i.e., to find how the quantities  $T^*$ ,  $\rho^*$ , and  $u^*$  depend on  $\alpha$ . Equation (3a) together with Eq. (3b) gives

$$u^* = \frac{1}{\rho^*} \approx \frac{1 - \sqrt{1 - 2(1 + \alpha)T^*/\mu}}{2} \quad (4)$$

Then, Eq. (4) substituted into Eq. (3c) yields a complicated and implicit function about  $T^*$ ,  $\alpha$ , and  $\mu$ . After analysis and comparison,

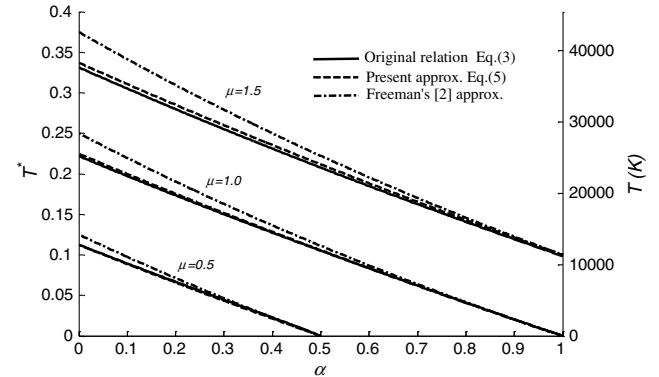


Fig. 2 Approximate relations between  $T^*$  and  $\alpha$  (nitrogen gas).

it is found that this implicit function could be approximately simplified to an explicit one, i.e.,

$$T^* \approx \frac{\mu - \alpha}{4.45 + 0.55\alpha} \quad (5)$$

which is a little different from that of Lighthill and Freeman's approximation but agrees more with the original Eq. (3c), as shown in Fig. 2. It is equivalent to first ignoring the kinetic energy behind the shock wave because  $u^{*2} \ll 1$ , and then regarding the undissociated molecules to be nearly fully excited in the vibrational degree of freedom. Equation (5) quantitatively indicates the reasonable redistribution of the total energy between the thermal mode and the chemical mode.

The next step is to build the rate equation of the chemical reaction. Consider the variation of the number density of  $N_2$ ,

$$\frac{\partial n_{N_2}}{\partial t} + \nabla \bullet (n_{N_2} \mathbf{v}) = \dot{\Omega}_{N_2} \quad (6)$$

In a one-dimensional steady flow, and considering that  $n_{N_2} = \rho_{N_2} / m_{N_2} = \rho(1 - \alpha) / m_{N_2}$ , Eq. (6) is simplified to

$$\frac{d\alpha}{dx} = - \frac{m_{N_2}}{\rho_\infty U_\infty} \dot{\Omega}_{N_2} \quad (7)$$

Theoretically speaking, the flow is completely described by Eq. (3) and (7). To solve this problem,  $\dot{\Omega}_{N_2}$  in Eq. (7) should first be expressed as a function of  $T^*$ ,  $\rho^*$ , and  $\alpha$ , and then Eqs. (4) and (5) are substituted into  $\dot{\Omega}_{N_2}$ . It finally leads to an ordinary difference equation of  $\alpha$ , which can be approximately integrated.

### III. DISSOCIATION-RECOMBINATION REACTION RATES

In this paper, the chemical reaction rates from the kinetic theory, instead of the engineering formulas, are employed to analyze the reactions. In Bird's monograph [12], it has been shown that the dissociation rate resulting from the collisions between species  $p$  and  $q$  takes the form of

$$k_f = \frac{2}{\sqrt{\pi}} \sigma_{\text{ref}} \left( \frac{T}{T_{\text{ref}}} \right)^{1-\omega} \left( \frac{2kT_{\text{ref}}}{m_r} \right)^{\frac{1}{2}} \times \left( 1 + \frac{1}{(3/2 - \omega + \bar{\zeta})T^*} \right) \exp \left( -\frac{1}{T^*} \right) \quad (8)$$

where the reduced mass  $m_r = m_p m_q / (m_p + m_q)$ ,  $\sigma_{\text{ref}} = \pi(d_p + d_q)_{\text{ref}}^2 / 4$ , and  $\bar{\zeta}$  denotes the mean value of the internal degrees of freedom in the collision. A molecule has two rotational degrees of freedom (DOF) and  $\zeta_v$  vibrational DOF, while an atom has no rotational or vibrational DOF. As a result, if  $p$  and  $q$  are both molecules,  $\bar{\zeta} = 2 + \zeta_v$ ; if one is a molecule and the other is an atom,  $\bar{\zeta} = (2 + \zeta_v)/2$ .

Theoretically, since the intermediate body can be either  $N_2$  or  $N$ , there should be two different dissociation rates, i.e.,  $(k_f)_{N_2+N_2}$ , owing

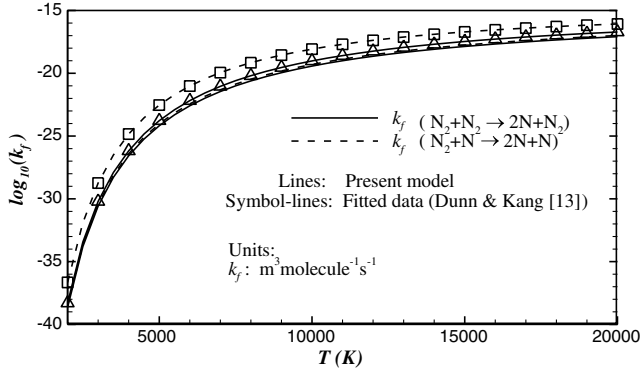


Fig. 3 Comparison between the present chemical reaction rates and the experimental data.

to collisions between molecules themselves, and  $(k_f)_{N_2+N}$  owing to collisions between atoms and molecules. It is found in the comparison that  $(k_f)_{N_2+N}/(k_f)_{N_2+N_2} \approx 1.5$ . To facilitate the subsequent analysis, these two rates could be combined into a single one, which means

$$k_f n_{N_2} n = (k_f)_{N_2+N_2} n_{N_2}^2 + (k_f)_{N_2+N} n_{N_2} n_N \quad (9)$$

where  $n_N = 2\alpha n/(1 + \alpha)$ ,  $n_{N_2} = (1 - \alpha)n/(1 + \alpha)$ , and the total number density  $n = (1 + \alpha)\rho/m_{N_2}$ . As a result,  $k_f = (k_f)_{N_2+N_2}(1 + 2\alpha)/(1 + \alpha)$ . In Freeman's work [2], the effects of the degree of dissociation did not appear in the dissociation rate, i.e., the correction factor  $(1 + 2\alpha)/(1 + \alpha)$  was roughly treated as a constant.

Now, the chemical reaction source term in Eq. (7) takes the form of

$$\dot{\Omega}_{N_2} = -[k_f n_{N_2} n - k_r n_N^2 n] \quad (10)$$

where the recombination rate  $k_r$  is derived from the equilibrium reaction theory but also holds for general nonequilibrium conditions. It means  $k_f/k_r = K_{eq} = \exp(-1/T^*)Q_N^2/(VQ_{N_2})$ , in which  $K_{eq}$  is the equilibrium constant and  $Q$  is the partition function [12] of a molecule or atom. Here, it will be convenient to introduce a characteristic density,  $\rho_d = m_{N_2}Q_N^2/(4VQ_{N_2})$ . Strictly speaking,  $\rho_d$  is a slowly varying function of the temperature. However, it was found [1] that the main features of the reaction are insensitive to the slight variation of  $\rho_d$ . As a result, a constant mean value could be employed within a specific temperature range. For the dissociation reaction of  $N_2$ ,  $\rho_d \approx 1.3 \times 10^5 \text{ kg/m}^3$  when  $T = 3000 \sim 10000 \text{ K}$ .

Figure 3 demonstrates a comparison between the reaction rates based on present model and the fitted data [13] used in engineering, which are consistent with each other in a large temperature range.

Now, Eq. (10) is substituted into Eq. (7), and, after some simplifications, it yields

$$\frac{d\alpha}{dx} \approx A \cdot C(\alpha) \cdot \left[ \exp\left(-\frac{1}{T^*}\right) - \frac{\rho_\infty \rho^*}{\rho_d} \frac{\alpha^2}{(1 - \alpha)} \right] \quad (11)$$

where  $A = 2(T_\infty/\theta_d)^{1/4}/(\sqrt{\pi}\lambda_\infty)$  and

$$C(\alpha) = \frac{[1 + (11/4 + \zeta_v)T^*](1 + 2\alpha)(1 - \alpha)}{(11/4 + \zeta_v)(T^*)^{3/4}u^{*2}\sqrt{\mu}} \quad (12)$$

Equation (11) is a complicated first-order differential equation of  $\alpha$  and  $x$ , with two main variable parameters  $\mu$  and  $\rho_\infty/\rho_d$ . Similar to what Freeman [2] has done, Eq. (11) could be numerically integrated for specific  $\mu$  and  $\rho_\infty/\rho_d$ . However, the numerical method only gives some discrete data points, and theoretical analysis is still very necessary for a more in-depth understanding of the flow mechanism.

#### IV. Equilibrium Degree of Dissociation

As mentioned above, at the place far enough downstream of the shock wave, the dissociation reaction will be counteracted by the recombination reaction, and both the chemical reaction and the flow

approach the equilibrium state. In Eq. (11), let  $d\alpha/dx = 0$ , and it gives

$$\exp\left(-\frac{1}{T_e^*}\right) = \frac{\rho_\infty}{\rho_d u_e^*} \frac{\alpha_e^2}{(1 - \alpha_e)} \quad (13)$$

where  $T_e^* = T^*(\alpha_e)$  and  $u_e^* = u^*(\alpha_e)$ . The left-hand side of Eq. (13) is an exponential-type function, whose significant variation could only result from the change of the order of magnitude of the right-hand side. Therefore, the slowly varying part of the right side of Eq. (13) could be approximately considered as a constant. As a result, it is reasonable and practical to employ an ensemble average of  $\rho_d u_e^*$  by introducing the characteristic free-stream density  $\rho_{d\infty} = \rho_d u_e^* \approx 1.0 \times 10^4 \text{ kg/m}^3$ . This treatment yields the following version:

$$\exp\left(-\frac{4.45 + 0.55\alpha_e}{\mu - \alpha_e}\right) = \frac{\rho_\infty}{\rho_{d\infty}} \frac{\alpha_e^2}{1 - \alpha_e} \quad (14)$$

Furthermore, when the equilibrium degree of dissociation is very low, for example  $\alpha_e < 0.1$ , the effects of the chemical reaction are also relatively unimportant; when the equilibrium degree of dissociation is very high, for example  $\alpha_e > 0.9$ , the present model has become somewhat unrealistic, and additional effects such as ionization and radiation should also be considered. In most of the practical problems with which we are concerned, there usually involves a moderate degree of dissociation, i.e.,  $0.1 < \alpha_e < 0.9$ . Thus, when  $\rho_{d\infty}/\rho_\infty$  ranges from  $10^4$  to  $10^9$ , a first-order Taylor expansion of Eq. (14) near  $\alpha_e = 0.5$  approximately yields an explicit expression:

$$\alpha_e \approx \frac{\mu + 0.011D - 0.39}{0.0015D^2 - 0.063D + 1.8} \quad (15)$$

where  $D = \ln(\rho_{d\infty}/\rho_\infty)$ . Of course, the form of the final result might not be unique if different levels of approximation are employed. A more complicated result could apply to a wider range, but Eq. (15) is good enough to deal with most of the situations in practice. It will be shown later that Eq. (15) effectively describes the roughly linear relation of  $\alpha_e$  and  $\mu$ , with the slope slightly increasing with the decreasing of the density.

#### V. Nonequilibrium Characteristic Scale

In the above section, the far-field equilibrium state has been clearly discussed. The next step is to find out how far the flow needs to go to approach the equilibrium state, i.e., to find the nonequilibrium characteristic scale  $x_e$ . Now, Eq. (11) is rewritten in a non-dimensional integrated form

$$x_e^* = \frac{x_e}{\lambda_\infty} = \int_0^{0.95\alpha_e} f(\alpha) \exp[h(\alpha)] d\alpha \quad (16)$$

where  $\alpha_e$  is calculated with Eq. (15) or Eq. (14),  $h(\alpha) = 1/T^*(\alpha)$ ,  $f(\alpha) = g(\alpha)/[C(\alpha)A\lambda_\infty]$ , and

$$g(\alpha) = \left[ 1 - \frac{\rho_\infty \rho^*}{\rho_d} \frac{\alpha^2}{(1 - \alpha)} \exp\left(\frac{1}{T^*}\right) \right]^{-1} \quad (17)$$

When  $\alpha = 0.95\alpha_e$ , it is found that  $g(\alpha) \approx 1.4$  for a large range of  $\mu$  and  $D$ .

The integrand of Eq. (16) grows exponentially within the integral interval, and so the integral near the extreme point of  $h(\alpha)$ , i.e.,  $\alpha = 0.95\alpha_e$ , contributes the majority of  $x_e^*$ . It means

$$x_e^* \sim \left. \frac{f(\alpha)}{h'(\alpha)} \exp[h(\alpha)] \right|_{\alpha=0.95\alpha_e} \quad (18)$$

If the remainder terms are also taken into account, a correlation factor equaling 1.25 should be added, which finally yields

$$x_e^* \approx 1.6 \left( \frac{\theta_d}{T_\infty} \right)^{1/4} \frac{T_e^{*2} \exp[1/T_e^*]}{C(0.95\alpha_e) |\partial T^*/\partial \alpha|_{\alpha=0.95\alpha_e}} \quad (19)$$

Equation (19) gives an explicit expression of the characteristic scale of the nonequilibrium flow behind the shock wave. Although it is ultimately determined by the free-stream conditions ( $T_\infty$ ,  $U_\infty$ , and  $\rho_\infty$ ), its form is still too complicated to show a clear dependency, and, due to the mathematical properties of Eq. (16), it even demands that  $\alpha_e$  should be first calculated with a relatively high accuracy. Therefore, further simplification is necessary to get a clear and direct relation between  $x_e^*$  and the free-stream condition. Actually, based on analysis and comparison of Eq. (19) with numerical results in the logarithmic coordinates, a first-order approximate formula is found to be expressed as

$$x_e = \lambda_\infty x_e^* \approx \frac{\lambda_\infty}{3800} \left( \frac{\theta_d}{T_\infty} \right)^{1/4} \left( \frac{\rho_{d\infty}}{\rho_\infty} \right)^{1/2} \exp \left( \frac{5}{\mu^{3/5}} \right) \quad (20)$$

$\lambda_\infty$  could be approximately calculated with  $(\pi/2)^{1/2} v_\infty / a_\infty$ , where  $v_\infty$  and  $a_\infty$  are the dynamic viscosity and the sound speed of the free stream, respectively.

## VI. Nonequilibrium Transient Process

Now, we have known the final equilibrium state and how far it needs to reach this state, but we still do not know the transient process whereby the flow transits from the initial state to the final state. Additionally, we also would like to know whether there exists a general similarity for all the flows under different free-stream conditions.

A strict solution to this problem relies on the indefinite integral of Eq. (11), which is almost impossible in practice. Alternatively, in this paper, a large series of results from the numerical integral and DSMC method are normalized and compared with each other, which leads to a simple expression to approximately describe the variation of the degree of dissociation from zero to its equilibrium value, i.e.,

$$\frac{\alpha}{\alpha_e} = \frac{(x/x_e)^s}{(x/x_e)^s + c} \quad (21)$$

Here, the constant  $c \approx 0.0526$  considering that  $\alpha = 0.95\alpha_e$  at  $x = x_e$ . And, strictly speaking, the index  $s$  should slightly decrease with increasing  $\mu$  or decreasing  $\rho_\infty / \rho_{d\infty}$ . When  $\mu = 0.4 \sim 1.2$  and  $\rho_{d\infty} / \rho_\infty \approx 10^4 \sim 10^9$ , it is found that  $s \approx 0.7 \sim 1.3$ . As a result,  $s = 1$  is roughly employed here if not specified, and more precise relations could be found in further studies if necessary.

Given  $\alpha = \alpha(x)$ , the nonequilibrium variation processes of other flow field quantities are then obtained immediately from Eq. (4) and (5).

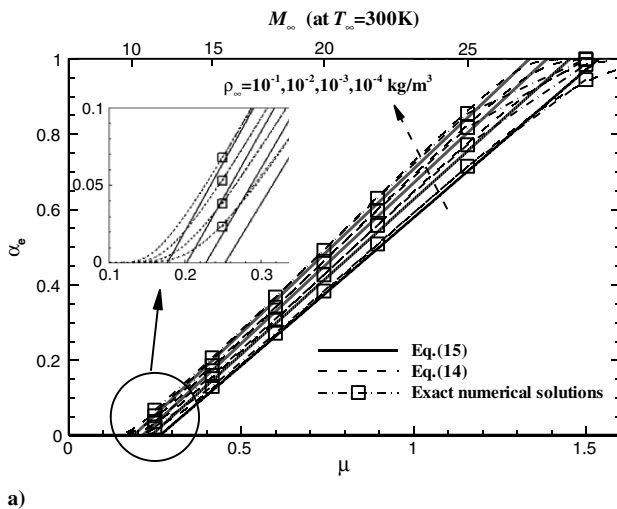


Fig. 4 The equilibrium degree of dissociation (nitrogen gas). a) Comparison between the present approximations and the exact numerical solutions. (b) Comparisons among the present approximation, Freeman's approximation, and the present DSMC results.

## VII. Results Validation and Discussions

To validate the theoretical analysis in this paper, the DSMC method is also used to simulate a series of cases in which  $\rho_\infty = 0.1 \sim 0.001 \text{ kg/m}^3$  and  $M_\infty = 15 \sim 25$  with  $T_\infty = 300 \text{ K}$  (corresponding to  $\rho_{d\infty}/\rho_\infty \approx 10^5 \sim 10^7$  and  $\mu = 0.416 \sim 1.15$ ). The present DSMC procedure employs the quantized vibrational levels and the vibration-dissociation coupling model [11,14,15] to simulate real gas effects. However, the ionization, radiation, and electronic excitation effects are not considered.

Figure 4 shows the variation of the equilibrium degree of dissociation under different conditions. Within the roughly linear interval  $0.1 < \alpha_e < 0.9$ , both the explicit formulation Eq. (15) and the implicit Eq. (14) match well with the exact numerical solution of the original conservation equations and strict rate equation without any mathematical approximation, which indicates that the present simplified model is a reasonable approximation to the original physical problem. The present DSMC results also compare well with the analytical predictions, with the maximum relative error less than 8%. After some numerical treatments, Freeman's approximation has also been shown in Fig. 4b. Both the present and Freeman's approximations overrate  $\alpha_e$  at the relatively higher values of  $\mu$ . In this region, as mentioned previously, more realistic models should be established.

The roughly linear relation between  $\alpha_e$  and  $\mu$ , as shown in Fig. 4, indicates the physical mechanism whereby, in the flows with moderate degrees of dissociation, nearly a constant proportion of the kinetic energy is transformed into the chemical energy via the dissociation reaction. It is also shown that a lower density results in a

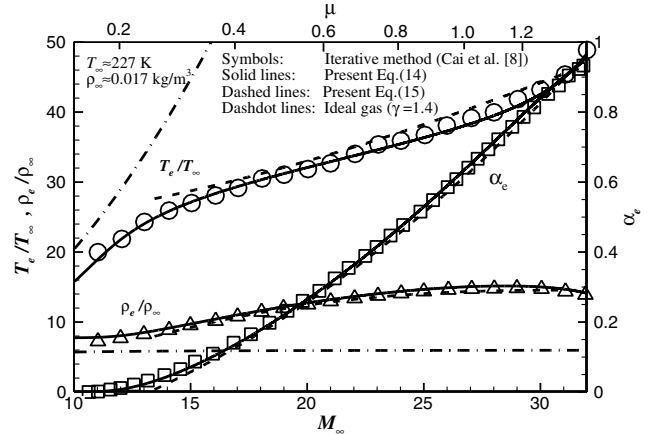
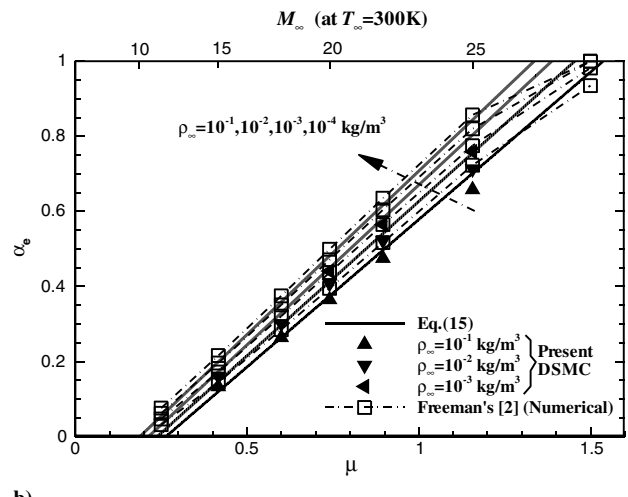


Fig. 5 The features of the equilibrium flow field (nitrogen gas).



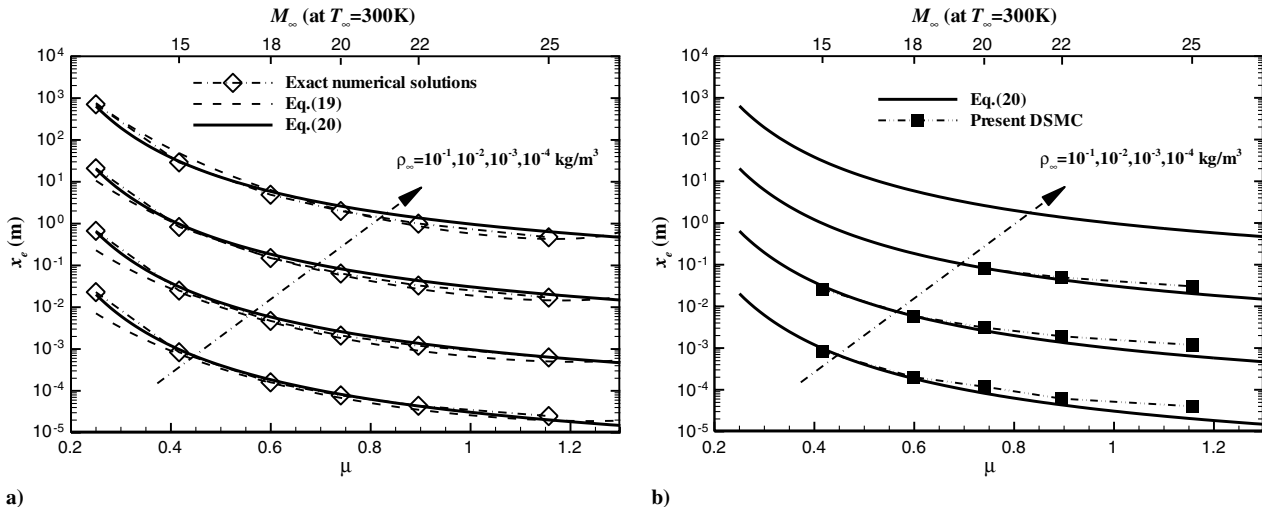


Fig. 6 The nonequilibrium characteristic scale (nitrogen gas). a) Comparison between the present approximations and the exact numerical solutions. b) Comparisons between the present approximation and the present DSMC results.

little higher equilibrium degree of dissociation. This feature could be explained from the microscopic mechanism whereby the recombination reaction involves triple collisions of molecules, and its probability is proportional to the cube of the density, whereas the dissociation probability is proportional to the square of the density.

Figure 5 shows features of the equilibrium flow field. The flow field predicted by the present analytical method agrees much well with Cai et al.'s result in [8], where the iterative method was used to solved the equilibrium flow and reaction equations. Their result is similar to the present exact numerical solution. Because of the significant real gas effects at high Mach numbers, the postshock temperature is drastically reduced and the postshock density rises higher relative to the ideal gas case.

Figure 6 shows the variation of the nonequilibrium characteristic scales under different conditions. Similarly, both the simple formulation Eq. (20) and the complicated Eq. (19) match well with the exact numerical solution within a large range of densities and kinetic energy. Now,  $\alpha_e$  in Eq. (19) has been calculated based on Eq. (15). As a result, Eq. (19) will lose its reliability at relatively lower values of  $\mu$ . In contrast, Eq. (20) is found to be still valid even at  $\mu = 0.25$ , where  $\alpha_e$  has been less than 0.1. The present DSMC results are also consistent with the analytical predictions within a certain accuracy, considering the drastically exponential variation of  $x_e$ .

At first glance, it is found that  $x_e^*$  is almost inversely proportional to  $\rho_\infty^{1/2}$ ; in other words,  $x_e \propto \rho_\infty^{-3/2}$ . For the case  $\rho_\infty = 0.1 \text{ kg/m}^3$ ,  $x_e^* \approx 10^1 \sim 10^3$ . Considering the relation between the mean free paths before and behind the shock wave, it could be estimated that, on

average, a nitrogen molecule approximately needs  $10^2 \sim 10^4$  collisions to produce the dissociation equilibrium. The higher the kinetic energy is, the less collisions it needs. When the density decreases, more collisions are needed, which may be due to the fact that the energy exchange efficiency in each single collision is lower in a more rarefied case, where the thermal nonequilibrium also becomes more and more significant.

Since the dissociation chemical reaction is very endothermic, it is foreseen that nonequilibrium characteristic scale must be intensively affected by the energy in the flow. Figure 6 shows that  $x_e$  varies very rapidly with  $\mu$ , which could hardly be predicted in the past.

The variation process of the degree of dissociation is shown in a normalized form in Fig. 7. The concise Eq. (21) catches the two main features, i.e., first a rapid increase and then a very slow approach. Although a higher  $\mu$  or a lower  $\rho_\infty/\rho_{d\infty}$  could result in a slightly steeper gradient near the shock wave, Eq. (21) is found good enough to describe most of the practical cases.

At last, the comprehensive comparisons for specific cases are demonstrated. In Fig. 8, good agreements are observed between the flow field predicted by the analytical method and the corresponding one from the present DSMC method. Moreover, experimental data [16] and some other numerical results [8] are also included in Fig. 9 to verify the present methods. Generally speaking, the main features of the nonequilibrium flow are well predicted, considering the uncertainties in the experiment and calculations. The slight discrepancies near the shock wave in Figs. 8 and 9 are due to the fact that the nonequilibrium of the molecular vibration is also entirely simulated in the numerical methods, whereas in the present analytical method

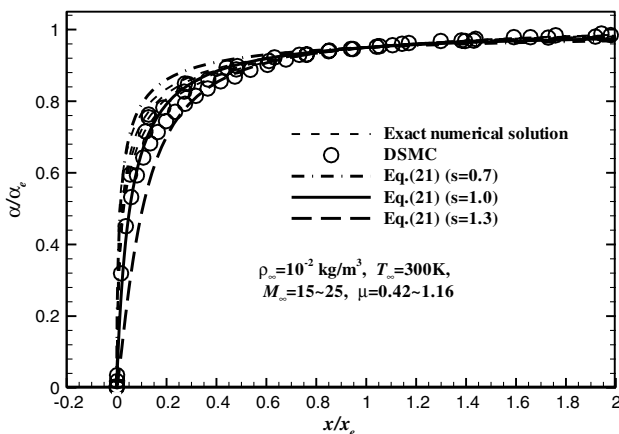


Fig. 7 The transient process of the degree of dissociation from zero to its equilibrium value (nitrogen gas).

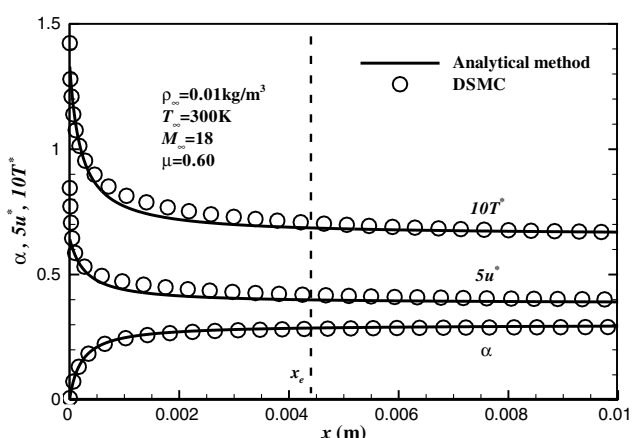


Fig. 8 The nonequilibrium flow behind the shock waves (nitrogen gas).

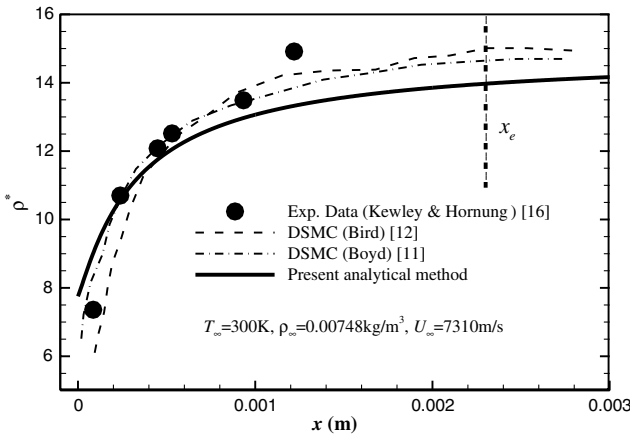


Fig. 9 Comparison of the density profile close to the shock wave (nitrogen gas).

the adoption of an ensemble approximate equilibrium to the molecular vibration leads to a relatively higher  $\rho^*$  but lower  $T^*$  and  $u^*$  at the original point.

In brief, the theoretical analysis and its conclusions are well verified by the present DSMC results, others' numerical results, and experimental data. The explicit formulations in this paper could apply to most of the practical flow problems, which involve a moderate degree of dissociation.

### VIII. Conclusions and Remarks

In this paper, the chemical nonequilibrium flow behind a strong normal shock wave was studied by using a theoretical modeling method. A dissociation-recombination reaction-rate equation based on the kinetic theory of molecules was built. After some appropriate simplifications and approximations, the explicit expressions of the equilibrium degree of dissociation and the nonequilibrium characteristic scale were given, i.e. Eq. (15) and (20), followed by a concise and normalized formula, Eq. (21), to describe the non-equilibrium transient process. These explicit formulations are valid in a large practical range of preshock state parameters. For the nitrogen gas flows, the free-stream velocity should range from approximately 4500 to 9000 m/s, and the density should range from  $10^0$  to  $10^{-5}$  kg/m<sup>3</sup>. The corresponding physical mechanisms were also discussed. Finally, the theoretical analyses and their conclusions were verified by the present and others' numerical results and available experimental data.

The present study yielded some significant analytical results about the nonequilibrium flow behind a strong normal shock wave, which could be helpful to enrich the theoretical framework of this classical problem. Moreover, the results in this paper could also be directly used in practice to quickly estimate and analyze the nonequilibrium flow field in CFD simulations, hypersonic wind tunnels, or flight experiments.

### Acknowledgments

This work was supported by the National Natural Science Foundation of China (Grant Nos. 90716011 and 91116012). The authors are very grateful to the reviewers for their valuable suggestions.

### References

- [1] Lighthill, M. J., "Dynamics of a Dissociating Gas. Part I: Equilibrium Flow," *Journal of Fluid Mechanics*, Vol. 2, No. 1, 1957, pp. 1–32. doi:10.1017/S0022112057000713
- [2] Freeman, N. C., "Non-Equilibrium Flow of an Ideal Dissociating Gas," *Journal of Fluid Mechanics*, Vol. 4, No. 4, 1958, pp. 407–425. doi:10.1017/S0022112058000549
- [3] Stalker, R. J., "Hypervelocity Aerodynamics with Chemical Nonequilibrium," *Annual Review of Fluid Mechanics*, Vol. 21, 1989, pp. 37–50. doi:10.1146/annurev.fl.21.010189.000345
- [4] Adamovich, I. V., Macheret, S. O., Rich, J. W., and Treanor, C. E., "Vibrational Relaxation and Dissociation Behind Shock Waves, Part 1: Kinetic Rate Models," *AIAA Journal*, Vol. 33, No. 6, 1995, pp. 1064–1069. doi:10.2514/3.12528
- [5] Adamovich, I. V., Macheret, S. O., Rich, J. W., and Treanor, C. E., "Vibrational Relaxation and Dissociation Behind Shock Waves, Part 2: Master Equation Modeling," *AIAA Journal*, Vol. 33, No. 6, 1995, pp. 1070–1075. doi:10.2514/3.48339
- [6] Wen, C., and Hornung, H., "Non-Equilibrium Recombination After a Curved Shock Wave," *Progress in Aerospace Sciences*, Vol. 46, Nos. 2–3, 2010, pp. 132–139. doi:10.1016/j.paerosci.2009.11.001
- [7] Cai, C., Liu, D. D., and Xu, K., "One-Dimensional Multiple-Temperature Gas-Kinetic Bhatnagar-Gross-Krook Scheme for Shock Wave Computation," *AIAA Journal*, Vol. 46, No. 5, 2008, pp. 1054–1062. doi:10.2514/1.27432
- [8] Cai, C., Khasavneh, K. R. A., Yang, S., and Lin, D. D., "A Gaskinetic Scheme for Nonequilibrium Planar Shock Simulations," *AIAA Paper 2009-0140*, 2009.
- [9] Kumar, S., Olivier, H., and Ballmann, J., "Numerical Study of Thermochemical Relaxation Phenomena in High-Temperature Non-equilibrium Flows," *Shock Waves*, edited by K. Hannemann and F. Seiler, Vol. 1, Springer-Verlag, Berlin, 2009, pp. 677–682. doi:10.1007/978-3-540-85168-4\_109
- [10] Boyd, I. D., "Analysis of Rotational Nonequilibrium in Standing Shock Waves of Nitrogen," *AIAA Journal*, Vol. 28, No. 11, 1990, pp. 1997–1999. doi:10.2514/3.10511
- [11] Boyd, I. D., "Analysis of Vibration-Dissociation-Recombination Processes Behind Strong Shock Waves of Nitrogen," *Physics of Fluids A*, Vol. 4, No. 1, 1992, pp. 178–185. doi:10.1063/1.858495
- [12] Bird, G. A., *Molecular Gas Dynamics and the Direct Simulation of Gas Flows*, 2nd ed., Clarendon Press, Oxford, 1994.
- [13] Dunn, M. G., and Kang, S. W., "Theoretical and Experimental Studies of Reentry Plasmas," NASA CR-2232, 1973.
- [14] Haas, B. L., and Boyd, I. D., "Models for Direct Monte Carlo Simulation of Coupled Vibration-Dissociation," *Physics of Fluids A*, Vol. 5, No. 2, 1993, pp. 478–489. doi:10.1063/1.858870
- [15] Knab, O., Fruhau, H. H., and Messerschmid, E. W., "Theory and Validation of the Physically Consistent Coupled Vibration-Chemistry-Vibration Model," *Journal of Thermophysics and Heat Transfer*, Vol. 9, No. 2, 1995, pp. 1070–1075. doi:10.2514/3.649
- [16] Kewley, D. J., and Hornung, H. G., "Free-Piston Shock Tube Study of Nitrogen Dissociation," *Chemical Physics Letters*, Vol. 25, No. 4, 1974, pp. 531–536. doi:10.1016/0009-2614(74)85360-1

S. Fu  
Associate Editor